CR 137744

Proposed NASA-CR

Preliminary Core-Engine Noise Abatement Experimental Results of a Fluid Injection Nozzle on a JT-15D Turbofan Engine

by

Dah Yu Cheng

and

Peter Wang

University of Santa Clara
Santa Clara, CA.

SUMMARY

Shear stress is the primary source of jet noise in a jet exhaust. The shear stress in a turbulent jet is equivalent to the rate of transverse momentum transport, which is also the cause of flow entrainment. If the surrounding fluid is injected radially inwards in order to reduce the work done for entrainment, then the local shear stress is reduced. From Lighthill's theory jet noise depends on velocity to the 8th power, hence, in a fan jet the majority of the noise is generated by the high velocity core jet.

To verify the inward momentum injection stress reduction concept, experiments were performed on a JT-15D Fan-jet engine such that the fan air is made convergently to flow around the high velocity core jet with a small angle.

Ring airfoils were used as flow separators for the minimization of the thrust loss. Jet exhaust noise reduction of 11 db at 30° from the jet axis was recorded and 8 db integrated overall noise reduction over a hemisphere was measured with only 4.6% thrust loss, or 152 db/percent thrust loss.

LIST OF SYMBOLS

M	Mach number
T	Temperature
Tij	i^{th} momentum in j^{th} direction
V	Velocity
p	Pressure
r	Radial dimension of aspherical coordinates
t	Time
u	Axial velocity component
v	Radial velocity component; volt
x	Axial coordinate
x_i	General coordinate in j^{th} direction
y	Radial coordinate of a cylindrical system
ϵ_0	Virtual kinematic viscosity
κ	Kinematic momentum
η	Dimensionless similarity coordinate,
ϕ	Strength of a source
Λ	Momentum diffusion length
ρ	Density

Subscripts

0	Stagnation condition
ex	Exhaust

Abbreviation

db	Decibel
rpm	Revolutions per minute
kg	Kilogram
m	Meter

k	Kelvin
Sec	Second
TSFC	Total specific fuel consumption

ABSTRACT

A noise suppression jet exhaust nozzle for a JT-15D fan jet engine was designed based on the momentum transport concept. The nozzle consists of a short thick lipped nozzle for the hot high velocity jet and is surrounded by multiple layers of fan air which was made to converging upon the hot core jet in order to simulate the jet entrainment streamlines. Reduction of the shear stress of the turbulent mixing is accomplished by suppressing the momentum transport rate in the radial direction. Ring air foils were used as flow separators in order to recover some of the thrust losses due to elongated fan duct. Both the noise reduction and thrust level were recorded at full power, 75%, and 50% RPMs of the inner core turbine. Test results indicated 11 db reduction is possible at full power. The integrated sound power was reduced up to 8 db at a thrust loss of 4.6% or 1.52 db/percent thrust loss.

INTRODUCTION

The majority of commercial airliners are powered by fan jets. The fan jet engine has good fuel economy and lower structural weight and cost compared to a conventional jet having the same thrust level. The awareness of noise pollution makes it necessary to find ways to reduce the jet engine noises. The noise generated by a fan jet comes largely from three sources: (1) fan (2) fan discharge duct and (3) primary jet (Fig. 1).

Various efforts have been devoted to understanding each of the noise sources. From Lighthill's jet noise theory (Ref. 1), the jet noise is proportional to the jet velocity to the 8th power. Due to temperature differences between the fan air and primary exhaust, the velocity of the primary exhaust usually is 40 percent higher than the velocity of the fan discharge. Therefore, the overall noise of the primary jet is about 15 db higher than that due to the fan discharge. If one can channel some of the fan air to mix with the primary jet so that the relative velocity can be reduced without the loss of integrated momentum, then the noise level ought to be reduced without substantial loss in thrust. Small co-axial jets have shown noise reduction up to 10 db in comparison with a single jet (Ref. 2 and 3) in both supersonic and subsonic conditions. The advantages of independently controlling the pressure ratio and mass flow rate of a laboratory-scale co-axial jet vanish when one is faced with the problem of quieting an existing fan jet engine with fixed performance characteristics and by-pass ratios. In this report, a co-axial jet nozzle is designed based on the knowledge of turbulent jet entrainment streamlines, to minimize thrust losses, and to maximize the noise reduction with a small penalty in structure weight. The nozzle design concept is based on the momentum transport theory formulated by Reichardt (Ref. 4). The entrainment flow obeys a similarity

solution such that the geometrical pattern of the flow streamlines are fixed in space independent of the jet velocity. This has also been experimentally verified in (Ref. 5). This leads to the possibility of mixing nozzle design in a wide range of engine throttling conditions.

Experimental results on sound level data based on momentum transport suppression concept of a JT-15D fan engine nozzle were obtained in angular distributed and single-array arrangements frcmnnear to far-field microphones. Thrust measurements were recorded by three load cells. The preliminary results show 11 db maximum off axis sound reduction and 8 db overall integrated sound power reduction. These test results provide a trend that high bypass ratio fan engine for wide body transport airplane can be extrapolated.

Theory of the Nozzle Design

From jet noise considerations, Lighthill's theory still provides the majcr guideline for subsonic nozzle design. The governing equation for jet noise production

$$\frac{\partial^2 \rho}{\partial t^2} - c^2 \nabla^2 \rho = \frac{\partial^2 T_{ij}}{\partial x_i \partial x_j} \qquad (1)$$

is a wave equation with a driving function

$$\frac{\partial^2 T_{ij}}{\partial x_i \partial x_j} \qquad (1.a)$$

If T_{ij} is a source-like function such that $T_{ij} \frac{\phi}{r}$ one can see from order of magnitude arguments, that $\frac{\partial^2 T_{ij}}{\partial x_i \partial x_j}$ will be a quadrupole function, $\frac{\phi}{\gamma^3}$.

To reduce noise becomes a search for a method of reducing this driving function $\frac{\partial^2 T_{ij}}{\partial x_i \partial x_j}$.

If one induces a momentum flux radially inward onto the hot core jet, in effect it reduces the work done by the hot core jet for entrainment. This

is equivalent to the reduction of the local shear stress. The gradient of the shear stress will be reduced as well. This process can be best seen from the momentum transport theory of Reichardt (Ref. 4). His original formulation was done in a two-dimensional system, extending Reichardt's physical reasoning to cylindrical jet is straight forward.

His basic equation is a time averaged momentum equation, that

$$\frac{\partial}{\partial x}\left(\frac{\bar{p}}{\rho} + \bar{u}^2\right) + \frac{\partial}{\partial y}\left(\overline{uv}\right) = 0 \qquad (2)$$

in a free turbulent flow, the laminar shear stress has been neglected. The pressure term vanishes for a subsonic jet and his second basic equation is of an empirical nature and has the form $\overline{uv} = -\Lambda \frac{\partial \bar{u}^2}{\partial y}$ (3)

Here $\Lambda = \Lambda(x)$ has the dimension of a length which usually is determined empirically. This is commonly known as the momentum transfer length. The left hand side of the equation represents the shearing stress, (except for the factor ρ,) which can be regarded as the quantity of the x component of momentum being transferred in the y-direction (flux of momentum). This relationship leads the momentum equation to a Fourier heat transfer equation.

$$\frac{\partial \bar{u}^2}{x} = \Lambda(x) \frac{\partial^2 \bar{u}^2}{\partial y^2} \qquad (4)$$

Equation (4) describes the x component of momentum diffusion in a free turbulent jet flow. If one injects some fluids along the entrainment streamlines in effect it is equivalent to reducing the x-momentum-transfer diffusion rate in the y-direction or a reduction in $\overline{uv}$. From the momentum equation it can be interpreted that the x component or jet momentum has to take longer distances to be dissipated in both the x and y-directions.

Nozzle Design

Since the performance of a JT-15D engine (Appendix I) can only be true if the engine is running at the factory specified conditions, one can see that the velocity ratio between hot core jet to the cold fan air is 40%. From the 8th power velocity dependence of jet velocity majority of the exhaust noise is from the hot core jet. The injection nozzle design is made to reduce the entrainment work or local shear stress of the high velocity core jet. The bypass fan air was made to flow in three convergent passages by ring airfoil separators. The geometrical shape of the ring airfoil were determined by matching the bypass nozzle area with the total throat area of the original engine, and the size of the ring airfoil flow separators were determined from similarity streamline analysis (Ref. 5). Subsonic jet streamlines can be calculated from incompressible flow consideration. Turbulent circular jet similarity velocity profiles are given as:

$$\text{axial} \qquad u = \frac{3}{8\pi} \frac{k}{\varepsilon_0 x} \frac{1}{(1+\frac{1}{4}\eta^2)^2} \tag{5}$$

$$\text{radial} \qquad v = \frac{1}{4} \frac{3}{\pi} \frac{k}{x} \frac{\eta - \frac{1}{4}\eta^3}{(1+\frac{1}{4}\eta^2)^2} \tag{6}$$

$$\text{where} \qquad \eta = \frac{1}{4} \frac{3}{\pi} \frac{k}{\varepsilon_0} \frac{y}{x} \tag{7}$$

and experimental evidence has shown that $\frac{\varepsilon_0}{k} = 0.0161$ for a turbulent jet. X is the axial direction and Y is the radial direction. The streamlines of the flow can be seen in Figure 2(a). The radial velocity v has two zero value points at, $\eta = 0$ and $\eta = 2$ (Fig. 2(b)). $\eta = 2$ corresponding to a straight line in x-y plane with an angle of 7.5° from the X-axis. This mathematical solution can be interpreted by following the physical reasoning

of jet entrainment, that a jet transports its momentum radially due to turbulent shear. The centerline velocity will be slowed down which forces the streamlines to be widened. This induces a radial velocity component outward. On the other hand, the entrained masses have a radial inward velocity. So somewhere in between the radial velocity vanishes, where the streamlines will be parallel to the jet axis. When a cylindrical wall intercepts this $v = 0$ line (Fig. 3), the effectiveness of the cylinder length to increase the entrainment mass flow ceases. This is the condition of determining the length of ring-airfoil flow separators.

From structure weight consideration, it is desirable to make this nozzle design as short as possible. If a nozzle is made to converge with an angle greater than 45°, then the interior of the nozzle would generate stationary vortices or known as the dead-water region. This normally produces a single tone noise as that of a whistle. For this investigation a 30° half angle was chosen for the core jet nozzle with a substantial fillet added to smooth out the transition. The lip of the nozzle was made blunt with a large radius (see Fig. 4). The thought behind the blunt lip design was that a sharp lip would create a single hanging vortex which would be the source of the edge tone sound noise. Ordinarily, the sharp lip is better when the nozzle is operated exactly at the design point. When a nozzle has to operate over a wide range of pressure ratios, the blunt lip creates a pair of vortices rotating in the opposite direction which creates a dipole like source. Although disturbances are more intense at near field, it can be attenuated more rapidly due to higher order sound effect. The dead water region behind the lip forms its own separation lines (Fig. 4), so in reality a fictitious sharp lip still exists with the shape varying according to the flow condition.

Two ring airfoils were chosen as by-pass flow separators. The ring

airfoils had a thickness-to-chord ratio of 10% for the first passage and 6% for the second and third passages respectively. The dimensions of the design can be seen in Fig. 5. The free expansion of the core jet of the JT-15D engine to the atmosphere has a Mach number of 0.665 at a local speed of sound for the specified exhaust temperature. The exhaust velocity can be slowed down slightly, when the exhaust plane pressure is increased due to the convergent fan-air-flow. This design allows the first stage mixing hot jet velocity to slow down to Mach number of 0.6. The expansion and mixing between the hot core jet and the by-pass air flow will not result in great thrust loss due to the law of conservation of momentum. The increased pressure by the radial component inward of the by-pass flow are used to determine the flow passage angles. From the supplied JT-15D engine data, the by-pass duct pressure is 1.45×10^5 Newtons/m^2, the exhaust flow to 1.07×10^5 N/m^2 reduced the Mach number from 0.775 to 0.7, at a velocity of 238 m/sec. The component of the cold flow velocity which causes the local pressure increment determines the first by-pass passage angle to be 23.50^o. The second and the third passages were determined from geometrical factors required for equal mass flow rates and the intersection point of $v = 0$ line.

Since the leading edge of the ring airfoil will not be in contact with any high temperature gases, the shaping of the curvature can be made by plastic foam and fiberglass cover in order to save construction cost and weight. The after body was made by two convergent thin sheet metal cones,forming a typical monocoque structure for light weight and maximum strength. The very outer nozzle has the struts attached to the ring airfoils as it forms a bicycle-wheel like structure. Again, very light material can be used to form a very strong and light weight structure without the problem of warpage as of single sheet nozzles. The total weight of this nozzle is about 50 kg using non-aluminum materials. The

dividing ring has a cross section of a reversed airfoil, such that the pressure loading of the ring produces force components in the thrust direction thus it can compensate some of the surface drag losses.

This three-passage nozzle system was found experimentally later having too low a fan pressure which causes fan RPM to hunt, therefore a second configuration is formed due to the restriction of allocated test period by blocking off a third passage (Fig. 5) with a metal cone and sound absorbing materials packed in the passage. Test results will be shown as having significant differences in the sound data.

Apparatus and Procedures

Experimental tests were conducted at Moffett Field early in the morning when background noise was low and the wind was calm. The test site located at least 600 km away from any big buildings (Fig. 6). The small trailer 30 km away from the engine is the operating room housing all the instrumentations.

Test Setup

The JT-15D engine was mounted on a stand 3.64 meters above the ground measured from the center line of the engine. This is made to avoid the local vortex attachment from the inlet to the ground and to reduce the reflection and interference of the noise data off the ground (Fig. 6). The engine thrust was measured by six strain gage type load cells at the mounting points. Forces in both the x and y directions were recorded to provide the data needed to compensate for the misalignment of the thrust vector to the engine stand. The engine running condition was based on inner turbine rpm measured in percentages, such as the idling condition, 50%, etc. During the experiment the engine was tested at 50%, 75%, and 92% rpm as standard comparison conditions. When the

engine was not moving in the stream, the 92% rpm required 100% hp output from the turbine because the original engine was designed to take into account the impact pressure from aircraft velocities. A bell mouth inlet was used throughout the test program.

Sound Measuring Equipment and Procedures

The sound data was tape recorded at 29 stations on the plane of the axis of the nozzle 3.64 meter above the ground (see Fig. 6) by 1.27 cm diameter Bruel and Kjaer condenser microphones, Type 4133, on an arc of 22.8 meter radius. Near field and very far field microphones were 1.016 meters and 36.5 m away, respectively. The position of each microphone station can be seen in Fig. 7.

Type 4133 B&K microphones with B&K Type 2619 preamplifier and matching cables were used to transmit signals to the B&K model 222-2 microphone energizer modules in the control room. The signals were tape recorded by an Ampex FR 1800L recorder/reproducer. The taping modes were FM modulated to give a frequency range of 0 to 300 kHz, depending on tape speeds (1-7/8, 3-3/4, 7-1/2, 15, 30, 60, and 120 inches per second). The data were recorded at 60 ips which was chosen for the optimum speed of the noise spectrum with a minimum quantity of the tape. Signal wave forms and amplitudes were simultaneously observed on a Tektronix oscilloscope, Model RM501A and HP 340DA RMS Voltmeter (see Fig. 8). The DC drift of the system is less than ± 0.5% of the total deviation over a four-hour period after warm-up.

The type 4133 B&K condenser microphone has a frequency range between 1 Hz to 40 KHz up to 160 db sound pressure level. With the type 2619 preamplifier the usable frequency is 2-200 KHz at 200 volt polarization voltage with an output of 12.5 mv/Newton/m^2. The nominal distortion is less than 1%, and the self generated noise between 20 KHz to 40 KHz is less than 40 μV.

The microphone, preamplifier, and energizer system was calibrated by means of piston-phone B&K type 4220, before each run at 124 db and a 250 Hz monotonic sound, which generates a microphone output of 0.5F rms to feed the recorder. Due to the ambient temperature fluctuation, a slight drift of less than $\pm$ 0.01 db was detected before and after the runs.

Data Reduction

Recorded data were analyzed by feeding the taped signals into a Spectral Dynamics Corp. real time spectrum analyzer, Model SD 301B, and into an SDC ensemble averager, Model 5D302A. A sixty-four ensemble-averaged output was displayed on a Tektronix oscilloscope, Type 7704A, and a Ballentine rms voltmeter, Model 320, simultaneously (Fig. 9).

The rms voltmeter reads the output of the ensemble averager. The system was calibrated by an audio frequency oscillator, again set at .5V for 124 db as a reference. Integration of the area of the spectrum range gives the overall sound power level. The total sound level of an engine can be obtained by integrating the sound pressure flux over a hemispherical surface 22.8 meters from the center.

Test Results

During the test it was found that the fan pressure could not meet the specifications supplied by the engine company. It was necessary to block passage 3 (Fig. 3) off in order to bring the fan pressure up to 3.1×10^3 N/m^2. Without blockage, the fan pressure was only at 5.84 N/m^2 at 92% rpm. As a result, the tests could be made in three configurations; namely, the original engine, the three by-pass flow nozzle, and the two by-pass flow nozzle. Sound pressure data at 92%, 75%, and 50% rpm were compared among the three

configurations, as shown in Figs. 10–15. Up to 11 db reduction at some microphone position are obtained. The two passage nozzle especially showed large noise reduction around the jet. The thrust data are shown in Table 1.

TABLE 1: Thrust at Various rpm's

Power Setting, %rpm	Original Engine	2 By-pass Nozzle	3 By-pass Nozzle
Inner Turbines	Thrust,Nm(lbs)	Thrust,Nm(lbs)	Thrust,Nm(lbs)
50%	862.4 (195)	1048.6 (236)	1999.2 (449)
75%	4057.2 (913)	3959.2 (891)	3841.6 (864)
92%	9800.0 (2204)	9349.2 (2103)	8859.2 (1992)

The percentage of thrust loss for the 2 by-pass nozzle is 4.6% and for the 3 by-pass nozzle is 9.6%. At a lower power setting the overall noise os the engine is small for all of the configurations. The multiple by-pass nozzles made a significant change in the sound level but not in thrust. At 92% rpm, the integrated sound level around the engine was 158.8 db at 22.8M away in the original engine configuration, 150.3 db for the 3 by-pass nozzle, and 151.8 db for the 2 by-pass nozzle.

Thus, the noise reduction at 92% becomes 0.89 db per percent thrust for the 3 by-pass nozzle at a fan pressure of 6.89×10^3 N/m^2 and 1.52 db per percent thrust loss for 3 by-pass nozzle at a fan pressure of 3.1×10^4 N/m^2. Where the original engine can obtain a fan pressure of 3.79×10^4 N/m^2 but should be 4.62×10^4 N/m^2 according to manufacturer's specification at 100% rpm. The significance of the test results to the physical nature of noise reduction mechanism is in the future extension to large wide body transport fan jet engines. Discussions of the results will be presented in the next section.

Discussion of Results

Fan-engines are usually quieter than turbo-jets, except the noise level of the large wide body transport aircraft engines are still higher than the level set by Federal Government. Noise sources of a fan-engine are many, and the most important one is the core engine noise. Due to the large relative velocity between fan-air and hot core exhaust, one can use fluid dynamic principle to reduce the noise. Most of the noise reduction nozzle designs are based on rapid mixup or entrainment to slow down the hot core exhaust velocity quickly, such as the multiple tubes, Daisy Shape and other induced mixing schemes. Those designs intend to quiet down the noise according to 8th power velocity rule of Lighthill. In the present test, the nozzle design is based on the reduction of shear stress or reducing the mixing rate of co-axial jet layers. The results in the last section indicated the success of noise reduction based on this new concept, however, it is by no means the optimum design for the future wide-body transport engines. In this section, the detail of the results will be critically examined, and future improvements are recommended.

The preliminary design with the 3-passage nozzle was made according to the full throttle in-flight data provided in the engine catalog. But the ground testing and engine running condition is far from what was expected. As a result the original 3-passage nozzle design causes too low a fan pressure, although large noise reduction was obtained, the thrust loss is also large, (9.6%). Besides, the fan rpm started to hunt, as a result, the last passage of the nozzle was forced to be blocked off. This brings the fan duct pressure up and the first 2 flow passages closer to what was calculated. Higher thrust was regained and better noise reduction was also obtained except around 70° away from the jet axis, the microphone data shown higher noise level. Re-examination of the noise distribution in Figure 10, showed the "ears" around

70° microphone may be caused by the single tone noise of the "dead water" region due to the blockage of the last flow passage (Fig. 16). The noise distribution data with and without the blockage can be seen in Fig. 17, that the front end noise of the two configurations is almost identical (from 110° - 180°), they are lower than the bare engine configuration due to lower fan pressure. The data at 0°, is not real because of the possible flow hitting the microphone directly. This can be identified from spectrum data between 0° and 20° (Fig. 18), that only low frequency spike appeared at 0° microphone. Due to the "ear" in the noise distribution, spectrum data of the bare engine, 2 passage and 3 passage nozzles are compared as shown in Fig. 19. The spectrum were 64 ensemble averaged such that the db output will not change with higher ensemble averages. The 2-passage nozzle (with blockage) showed a single tone spike at 2,700 Hz which is more than 20 db above the white noise contributed by real jet noise. Thus the source of the "ear" sound is identified. If the last passage can be completely removed, not only the single tone sound can be eliminated but also the structure weight of the nozzle can be substantially reduced. This will be considered in future tests.

During this test, not only the sound reduction of a fan-engine is desirable but also the physics of slow down the jet mixing principle can be examined. Since in any jet the velocity is eventually dissipated, rapid dissipation increases the shear stress and noise, slow dissipation reduces the local shear stress but it elongates the potential core or enlarged sound production volume. To examine the effectiveness of this nozzle design, noise decay from near field to far field noise were examined as shown by microphone array along 30° off jet axis (Fig. 20). The almost constant noise level at full throttle extending to longer distances but at lower noise level for the 2 passage nozzle clearly indicate the shear stress reduction and the elongation of the potential core.

Any separator surfaces in a flow passage will cause drag losses. The ring airfoil design as the flow separators were intended to minimize the losses by regaining some thrust. From the flow geometry, one can find high pressure on the back side of the separator and low pressure on the curved side of the separator, thus creating a force component in the thrust direction. This was used to compensate some of the drag loss on the surface of separators. Pressure distribution measurements were made on ring airfoils from data shown in Figure 21, at low thrust loss for nozzle design can be understood.

Concluding Remarks

The performance of the fluid momentum injection nozzle design is based on the hypothesis that the reduction in local shear stress would result in extension of potential core and quieting the jet exhaust noise. The microphone data from the near field extending to far field indicated that regardless of the noise distribution at near field, far field noise can distinguish the merits of different nozzle designs; however, the 3-passage nozzle has a lower near field sound but extends to longer distances than that of the 2-passage nozzle. This confirms that the potential core of the jet was elongated and radiated at a lower noise level. The rapid decay at near field for the 2-passage nozzle also reflects the concept of thick lip nozzle for higher order sound.

The nozzle test results are very encouraging in that a theoretical argument based on momentum transport theory has been proven qualitatively in experiments. The nozzle weight and geometrical length were comparable to the original nozzle. Although over an 8 db noise level was recorded with less than 5% thrust loss, the test was disappointing in that the engine data supplied by the manufacturer was not the condition operated on the test stands. Better results can be expected with properly matched nozzles in the future. This type of noise

suppression design is expandable to larger fan jets. The weight of the nozzle can be further r·.duced with proper considerations in structure, strength, and weight.

REFERENCES

1. Lighthill, J. J.: Jet Noise, AIAA Journal, Vol. 1, July 1963, pp 1507-1517.

2. Dosanjh, D. S., Abdelhamid, A. M. and Yu, J. C., NASA SP-207, pp 63-101, 1969.

3. Plumblee, H. E., NASA SP-207, pp 113-136, 1969.

4. Schlitchting, H., "Boundary Layer Theory," McGraw-Hill, Inc. 6th Ed. p 702, 1968.

5. Schlitchting, H., "Boundary Layer Theory," McGraw-Hill, Inc., 6th Ed. p

6. Cheng, D. Y., Wang, P., and Chisel, D. M., Journal of Aircraft 10, No. 9, pp 569-570, September 1973.

FIGURE TITLES

1. Turbofan-engine noise emission.
2. Velocity streamlines (a) and profiles (b) of a circular turbulent jet.
3. Geometrical length determination of the bypass flow separator.
4. Convergence angle and the vortex structure of a blunt lip nozzle.
5. Dimensions of momentum - injection nozzle.
6. Engine stand, trailer and near field microphones.
7. Microphone positions.
8. Recording system layout.
9. Data playback system setup.
10. 92% rpm sound pressure between bare engine and 2-passage nozzles.
11. 92% rpm bare engine and 3-passage nozzles.
12. 75% rpm bare engine and 2-passage nozzles.
13. 75% rpm bare engine and 3-passage nozzles.
14. 50% rpm bare engine and 2-passage nozzles.
15. 50% rpm bare engine and 3-passage nozzles.
16. Blockage and possible dead water region of the nozzle.
17. Noise distribution at 92% rpm with and without blockage of the nozzle.
18. Spectral distribution of jet noise at 0° and 20° from the exhaust axis for 2-passage nozzle.
19. Spectral distribution of jet noises for three nozzle configurations at 92% rpm and from 50°, 60°, 70° and 80° microphone positions.
20. Comparison of noise decay profiles towards far field.
21. Pressure distribution at the inner surfaces of the ring airfoil flow separators.

TURBOFAN-ENGINE NOISE EMISSION

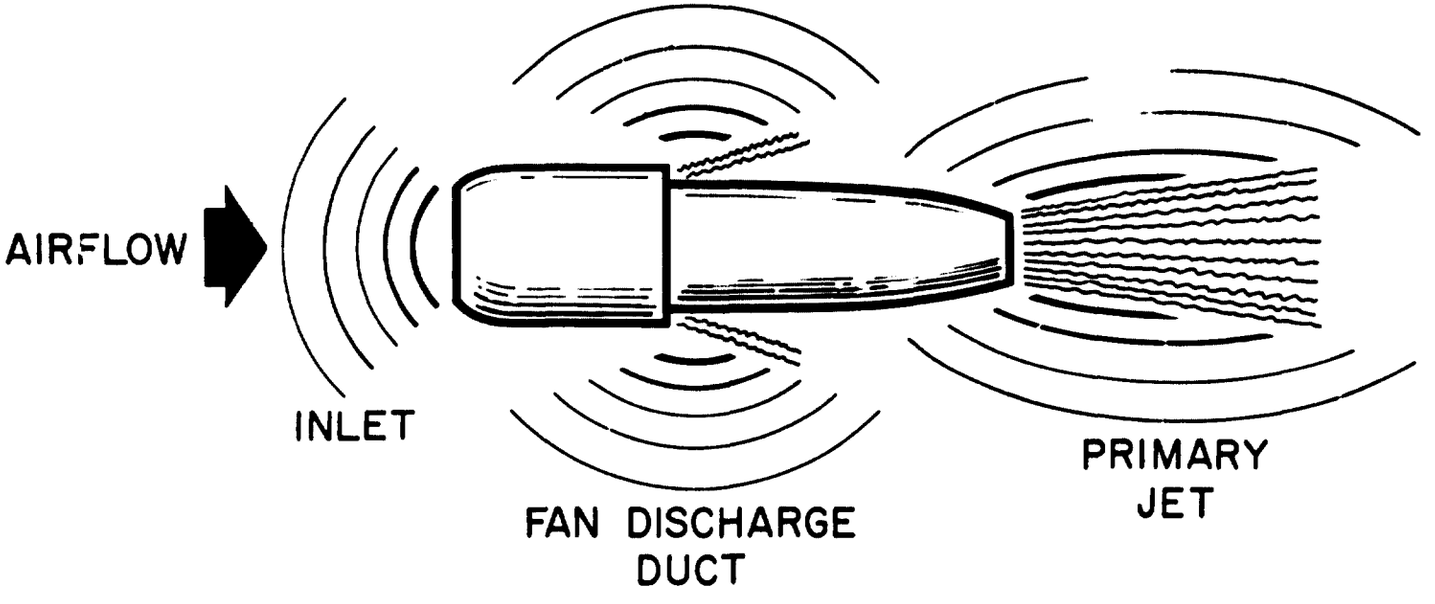

NATIONAL AERONAUTICS AND SPACE ADMINISTRATION
AMES RESEARCH CENTER MOFFETT FIELD CALIFORNIA

(a)

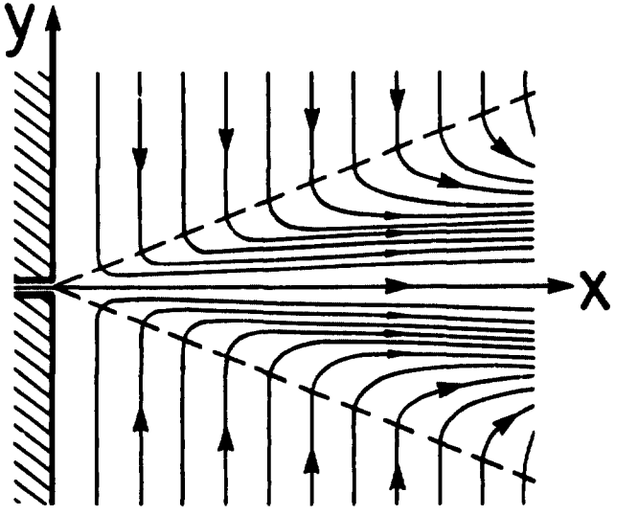

(b)

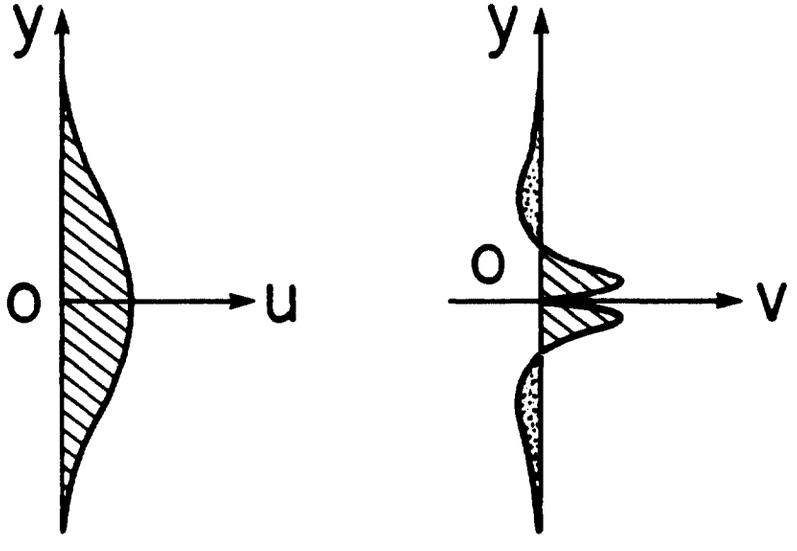

NATIONAL AERONAUTICS AND SPACE ADMINISTRATION
AMES RESEARCH CENTER MOFFETT FIELD, CALIFORNIA

PASSAGES

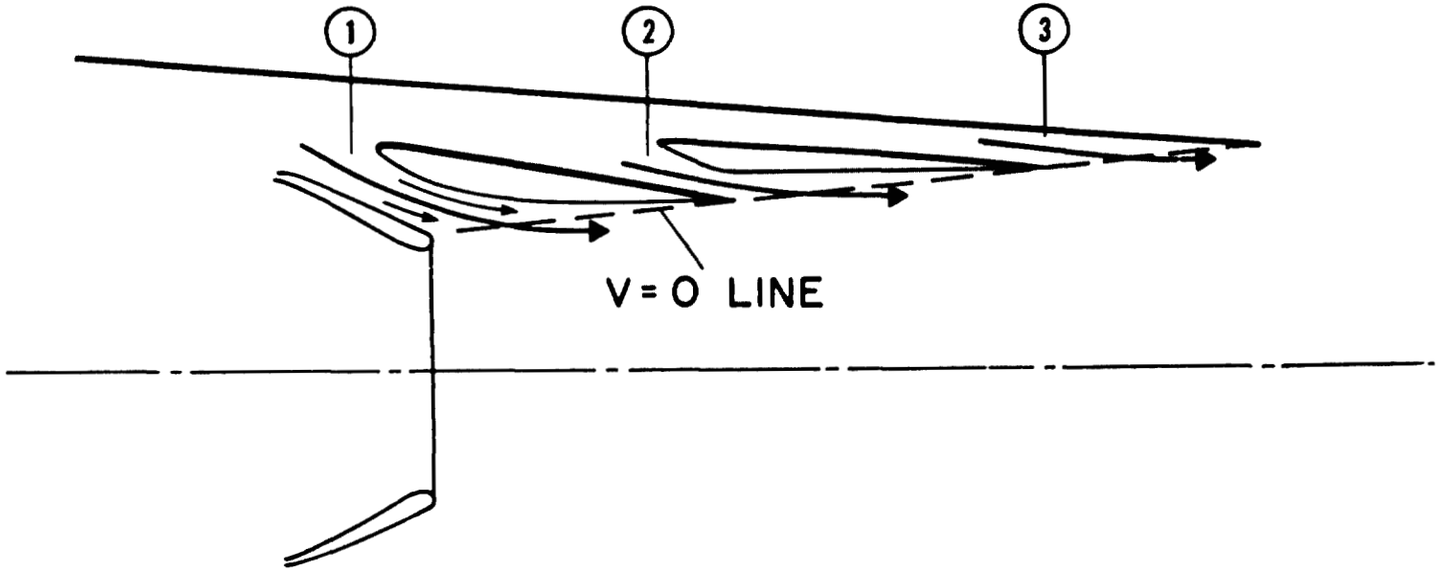

NATIONAL AERONAUTICS AND SPACE ADMINISTRATION
AMES RESEARCH CENTER MOFFETT FIELD CALIFORNIA

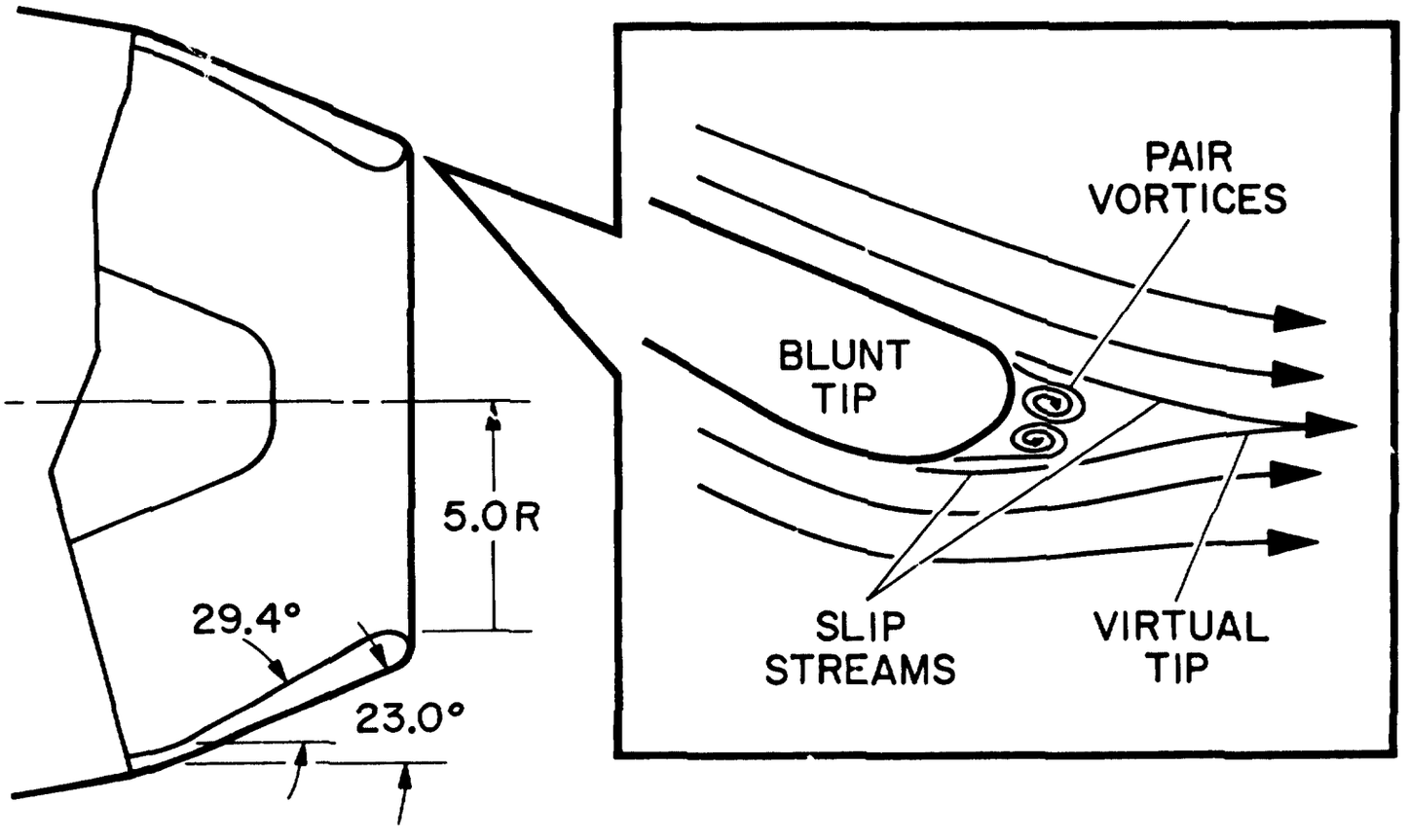

NATIONAL AERONAUTICS AND SPACE ADMINISTRATION
AMES RESEARCH CENTER MOFFETT FIELD, CALIFORNIA

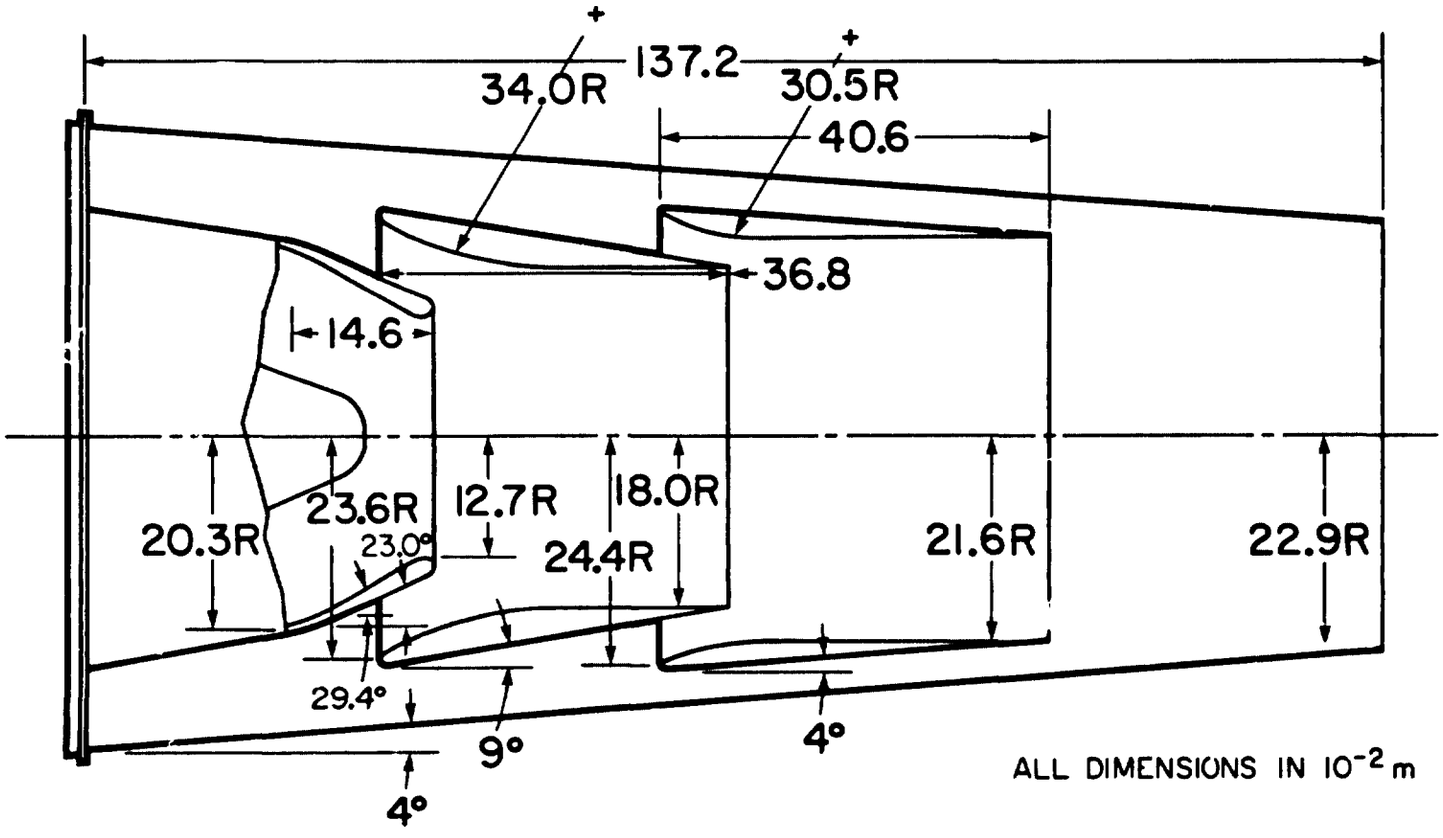

ALL DIMENSIONS IN 10^{-2} m

NATIONAL AERONAUTICS AND SPACE ADMINISTRATION
AMES RESEARCH CENTER MOFFETT FIELD CALIFORNIA

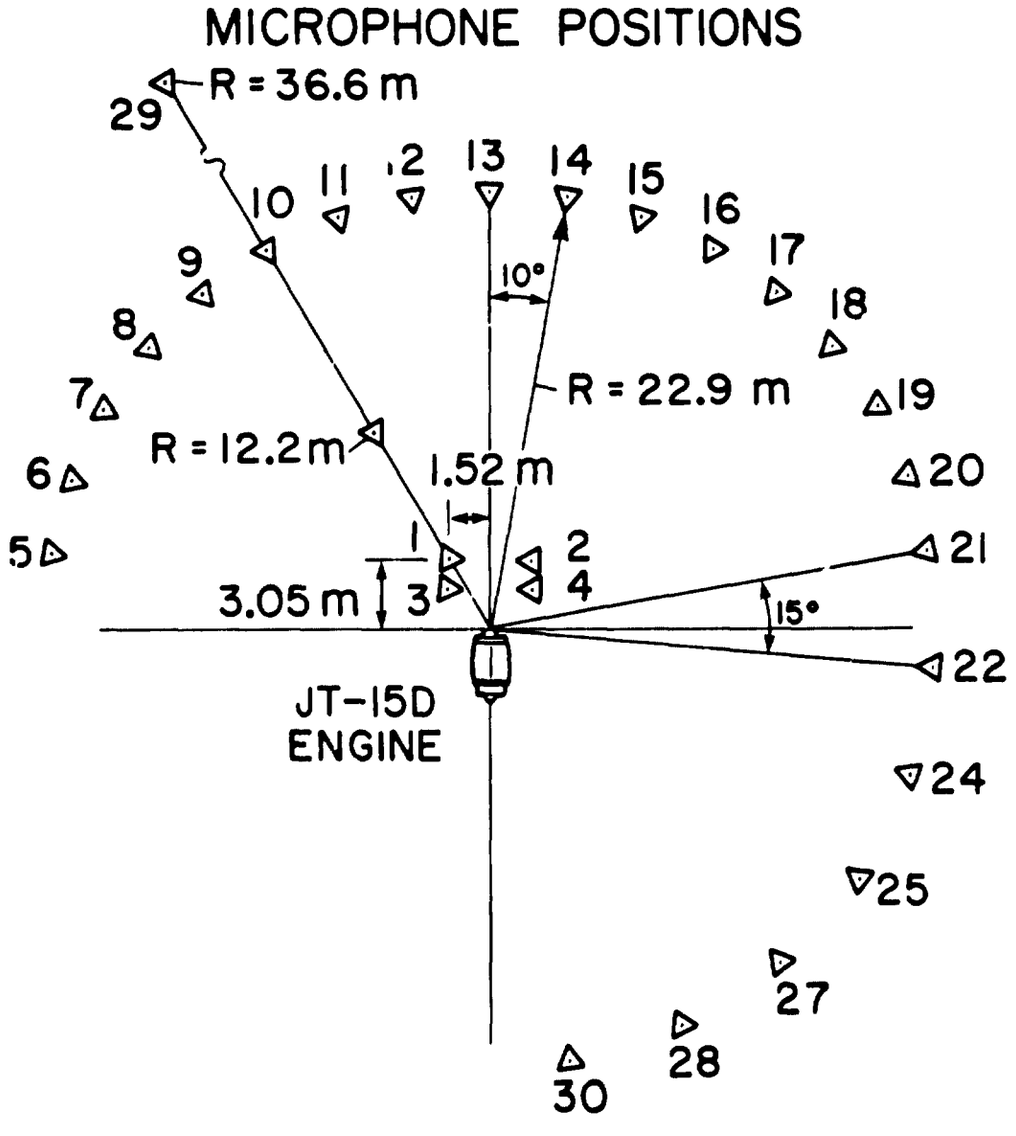

NATIONAL AERONAUTICS AND SPACE ADMINISTRATION
AMES RESEARCH CENTER MOFFETT FIELD CALIFORNIA

RECORDING SETUP

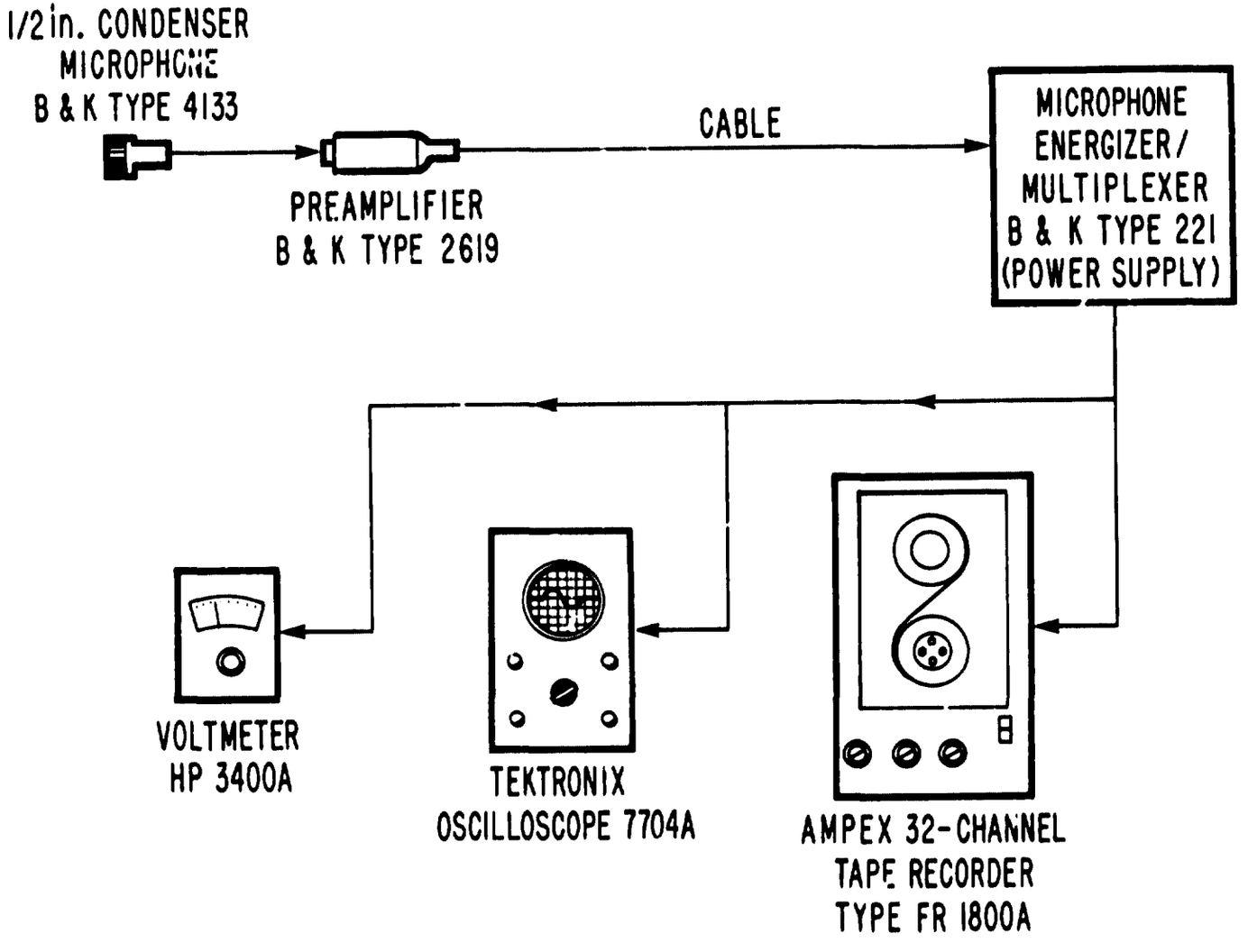

NATIONAL AERONAUTICS AND SPACE ADMINISTRATION
AMES RESEARCH CENTER MOFFETT FIELD CALIFORNIA

DATA REDUCTION BLOCK DIAGRAM

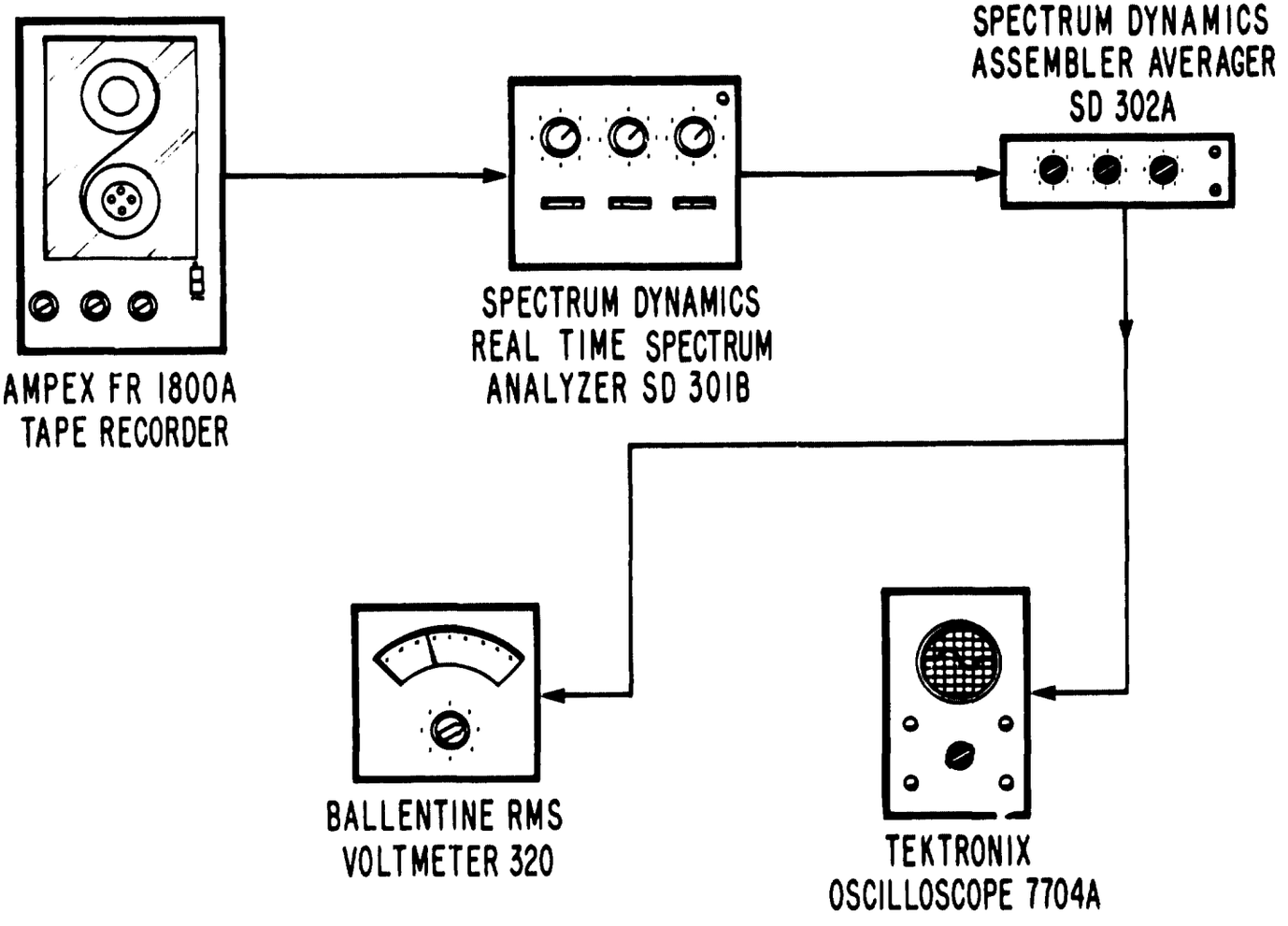

NATIONAL AERONAUTICS AND SPACE ADMINISTRATION
AMES RESEARCH CENTER MOFFETT FIELD CALIFORNIA

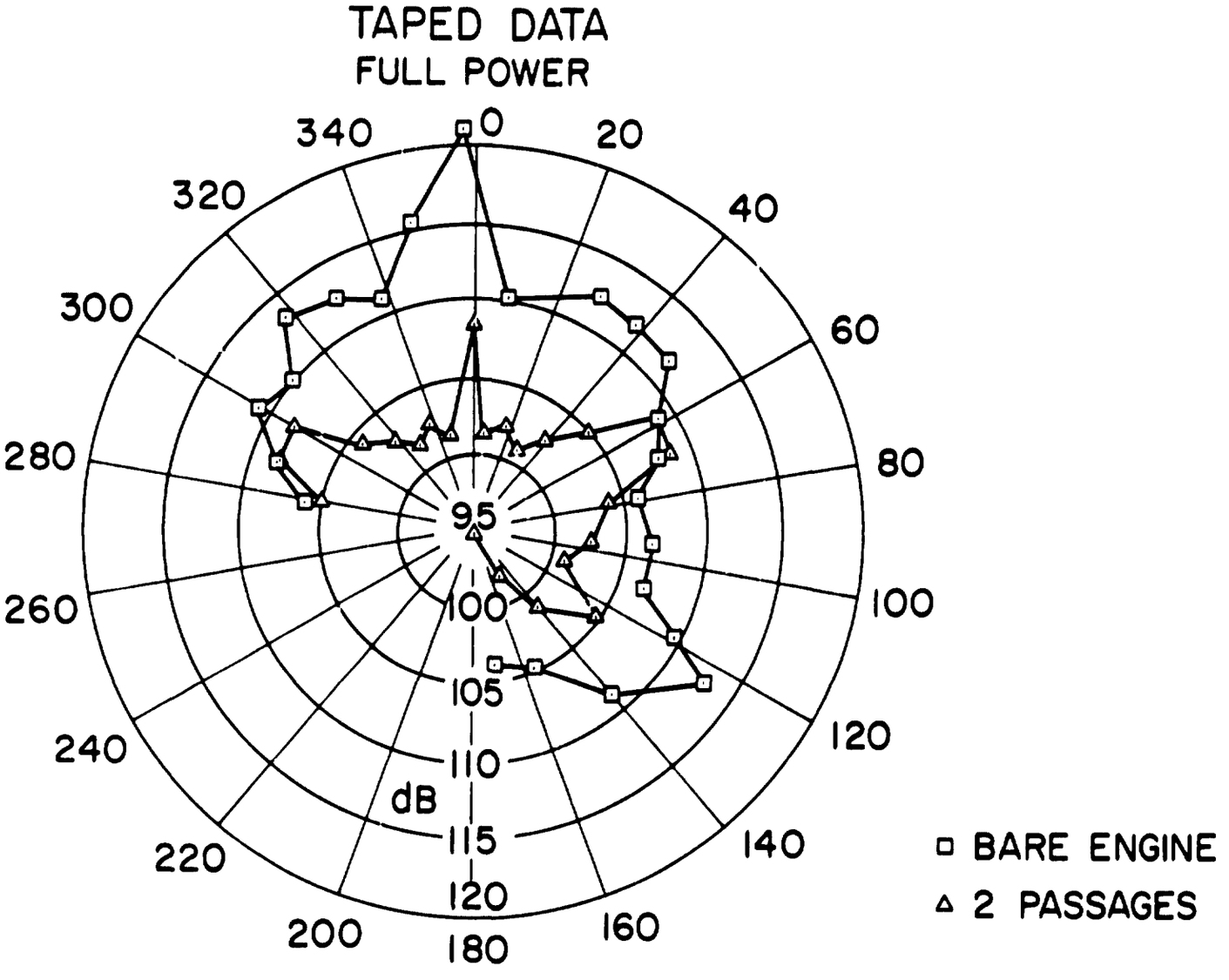
TAPED DATA
FULL POWER
0
20
40
60
80
100
120
140
160
180
200
220
240
260
280
300
320
340
95
100
105
110
115
120
dB
BARE ENGINE
2 PASSAGES

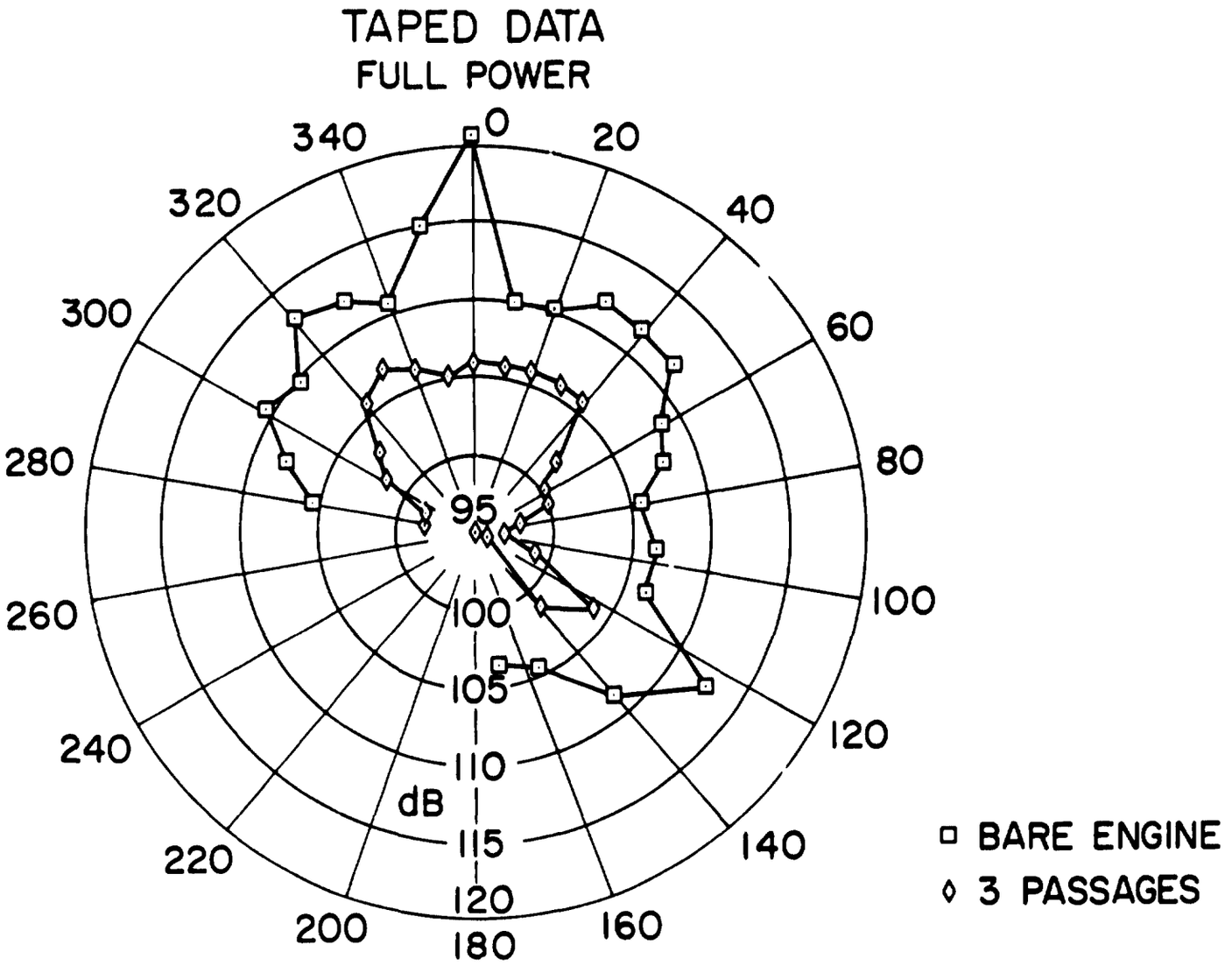
TAPED DATA
FULL POWER
0
20
40
60
80
100
120
140
160
180
200
220
240
260
280
300
320
340
95
100
105
110
115
120
dB
BARE ENGINE
3 PASSAGES

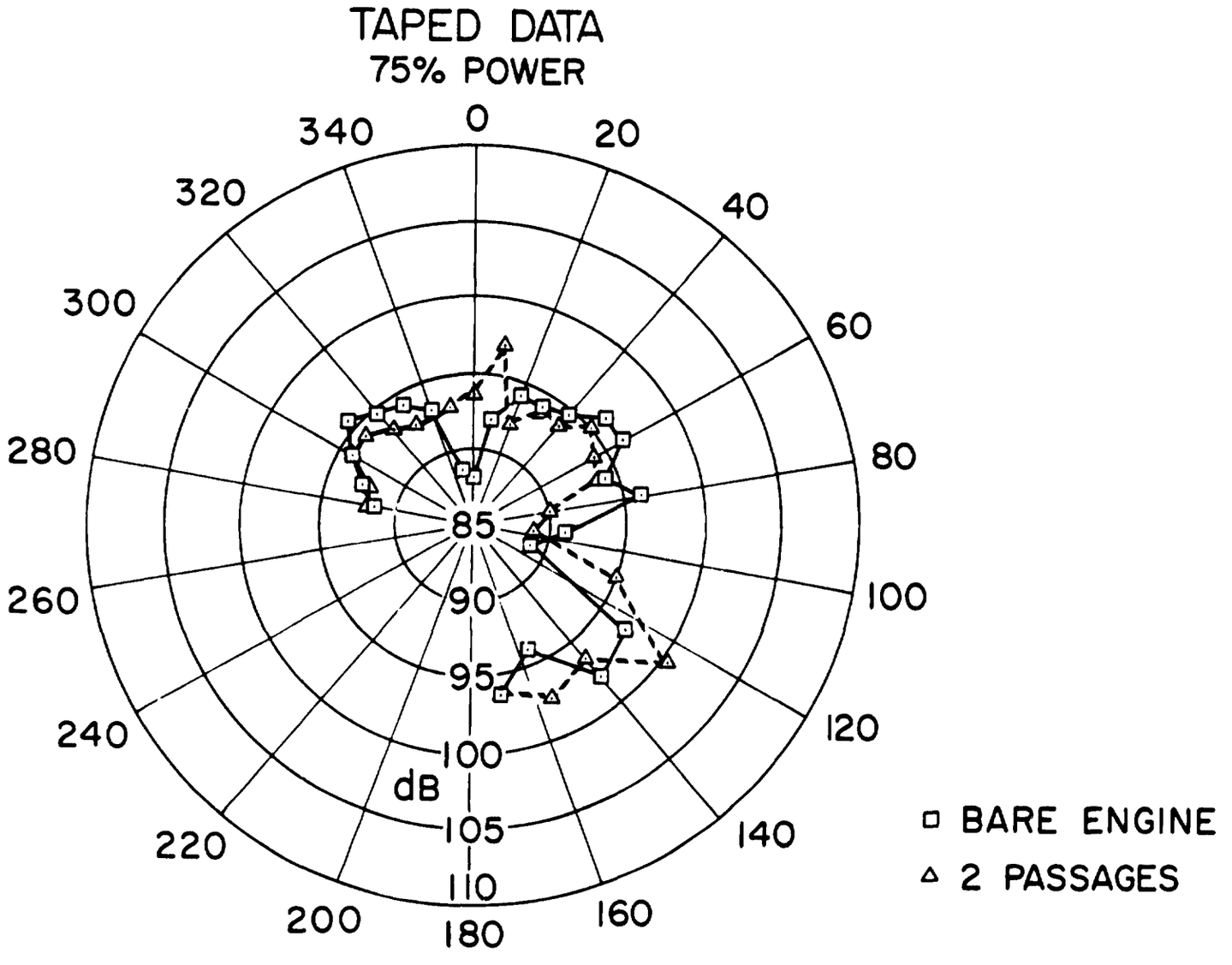

NATIONAL AERONAUTICS AND SPACE ADMINISTRATION
AMES RESEARCH CENTER MOFFETT FIELD CALIFORNIA

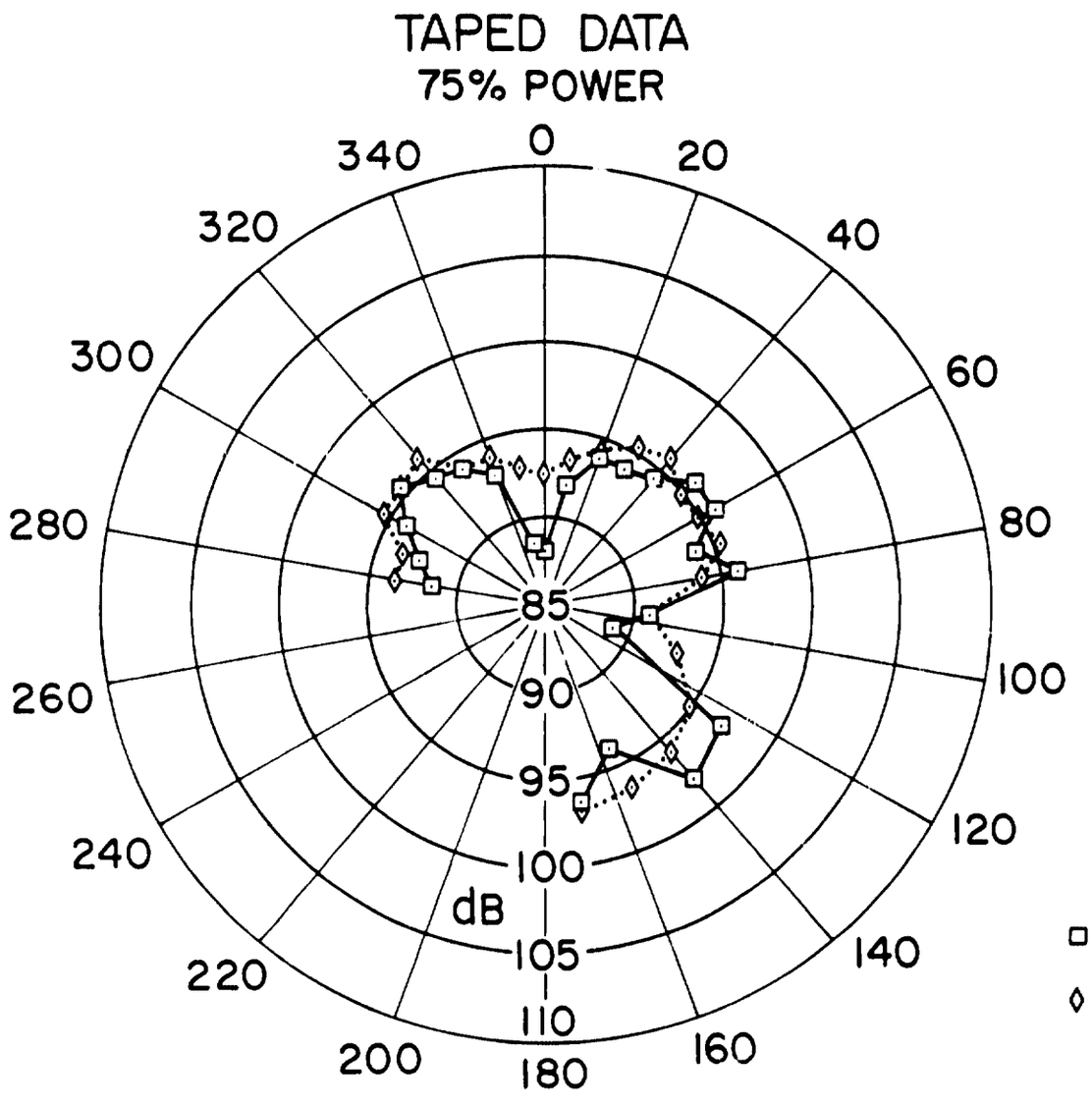

NATIONAL AERONAUTICS AND SPACE ADMINISTRATION
AMES RESEARCH CENTER MOFFETT FIELD CALIFORNIA

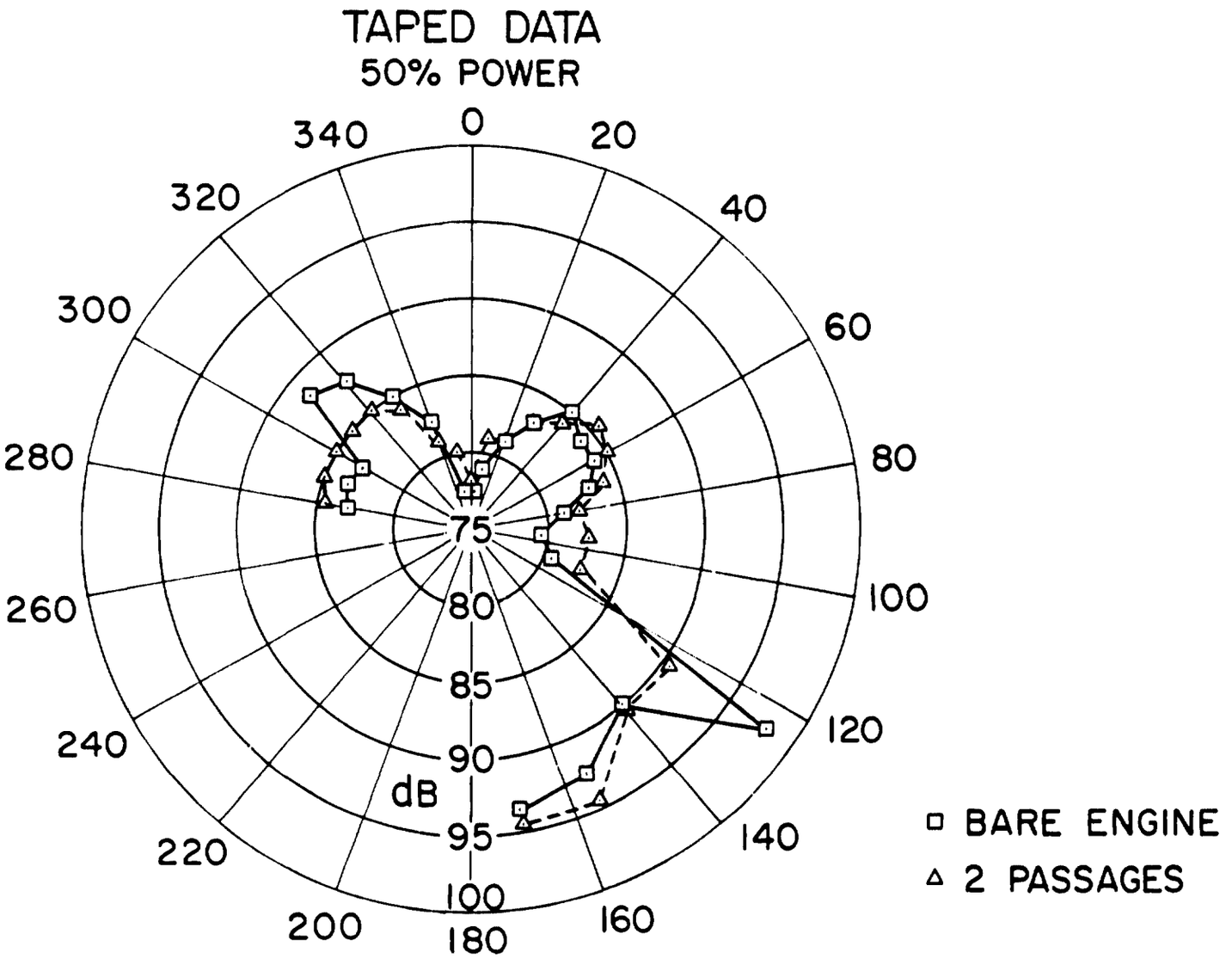

NATIONAL AERONAUTICS AND SPACE ADMINISTRATION
AMES RESEARCH CENTER MOFFETT FIELD CALIFORNIA

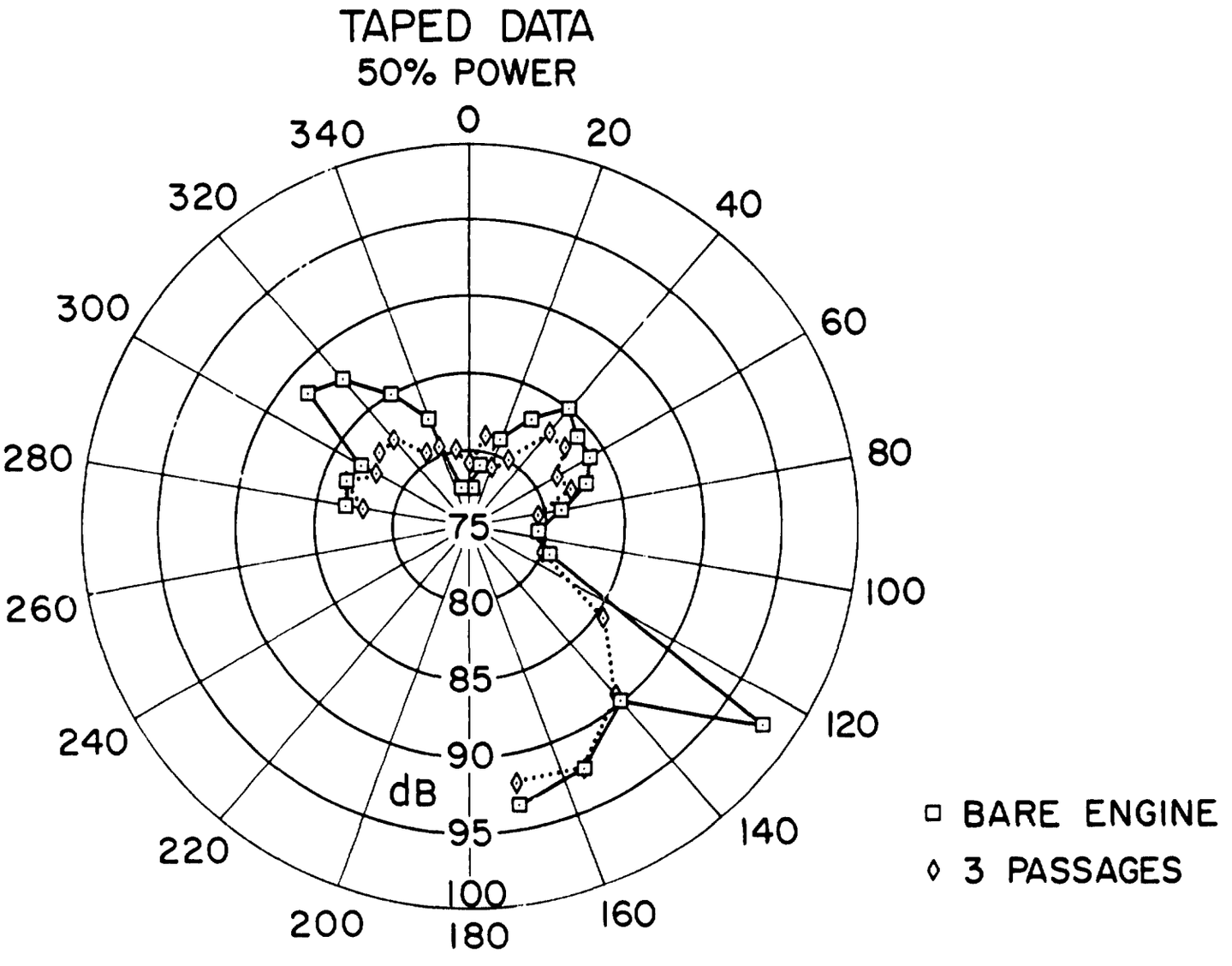

NATIONAL AERONAUTICS AND SPACE ADMINISTRATION
AMES RESEARCH CENTER MOFFETT FIELD CALIFORNIA

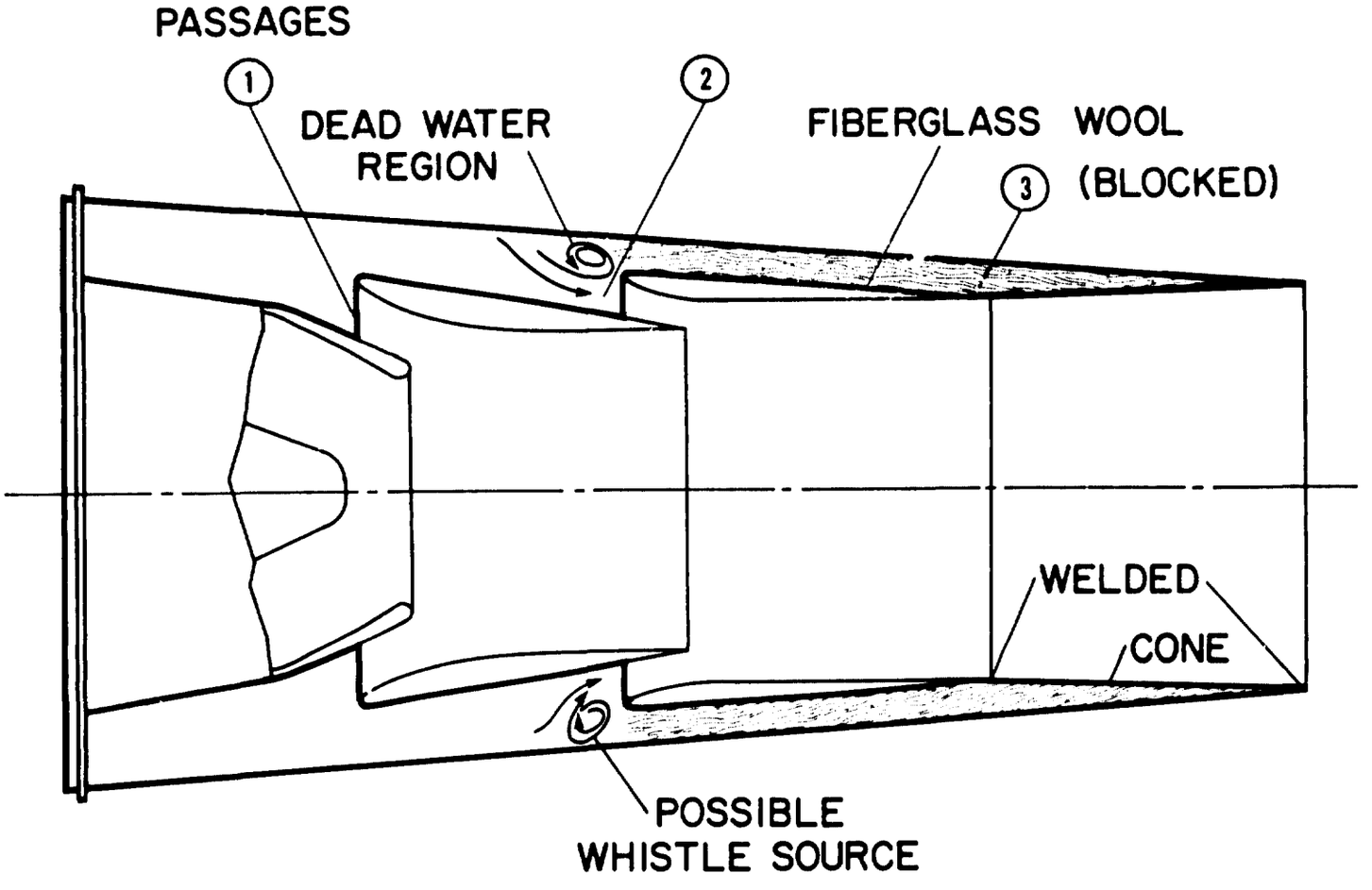

NATIONAL AERONAUTICS AND SPACE ADMINISTRATION
AMES RESEARCH CENTER MOFFETT FIELD CALIFORNIA

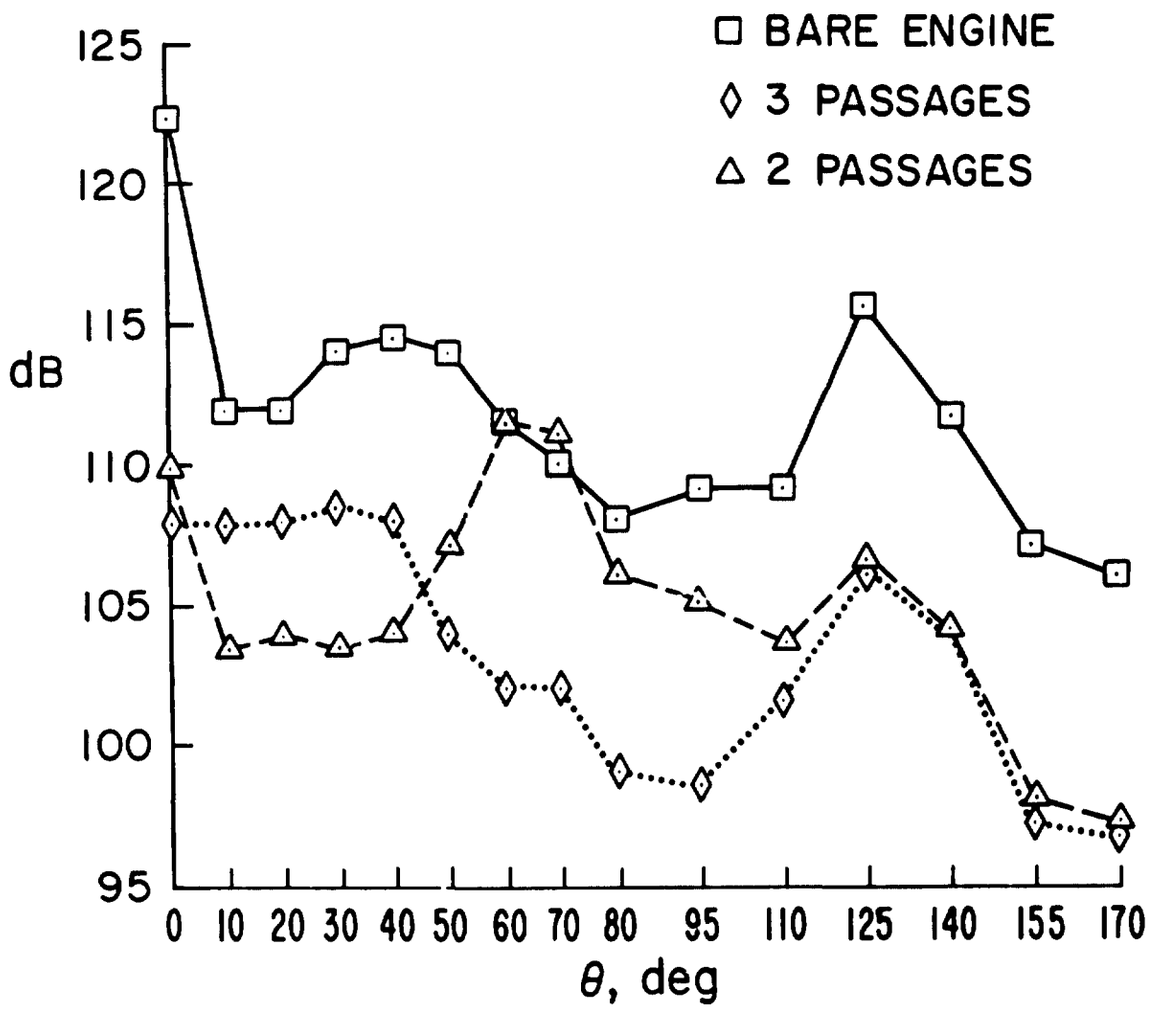
BARE ENGINE
3 PASSAGES
2 PASSAGES
125
120
115
110
105
100
95
dB
0 10 20 30 40 50 60 70 80 95 110 125 140 155 170
θ, deg

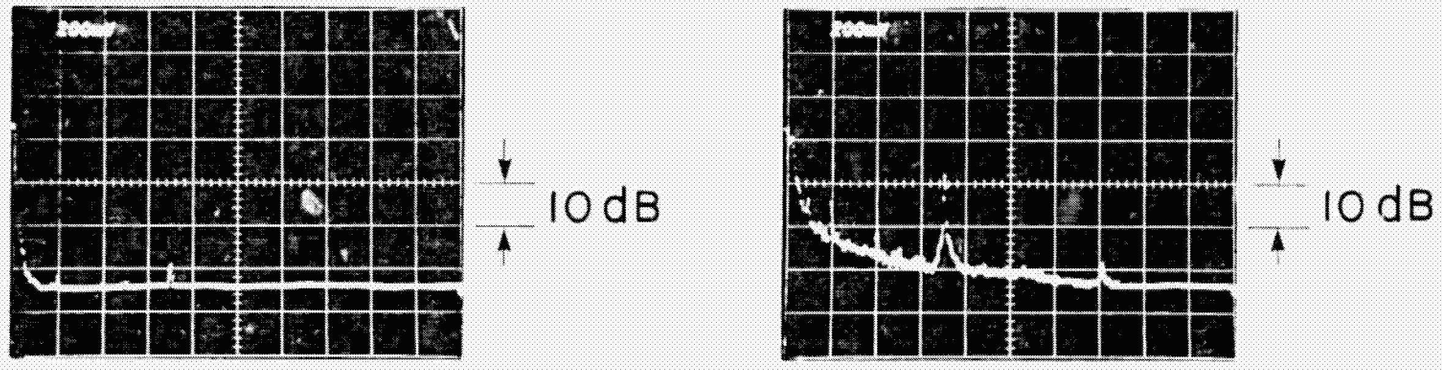

0°

20°

BARE ENGINE 92% RPM

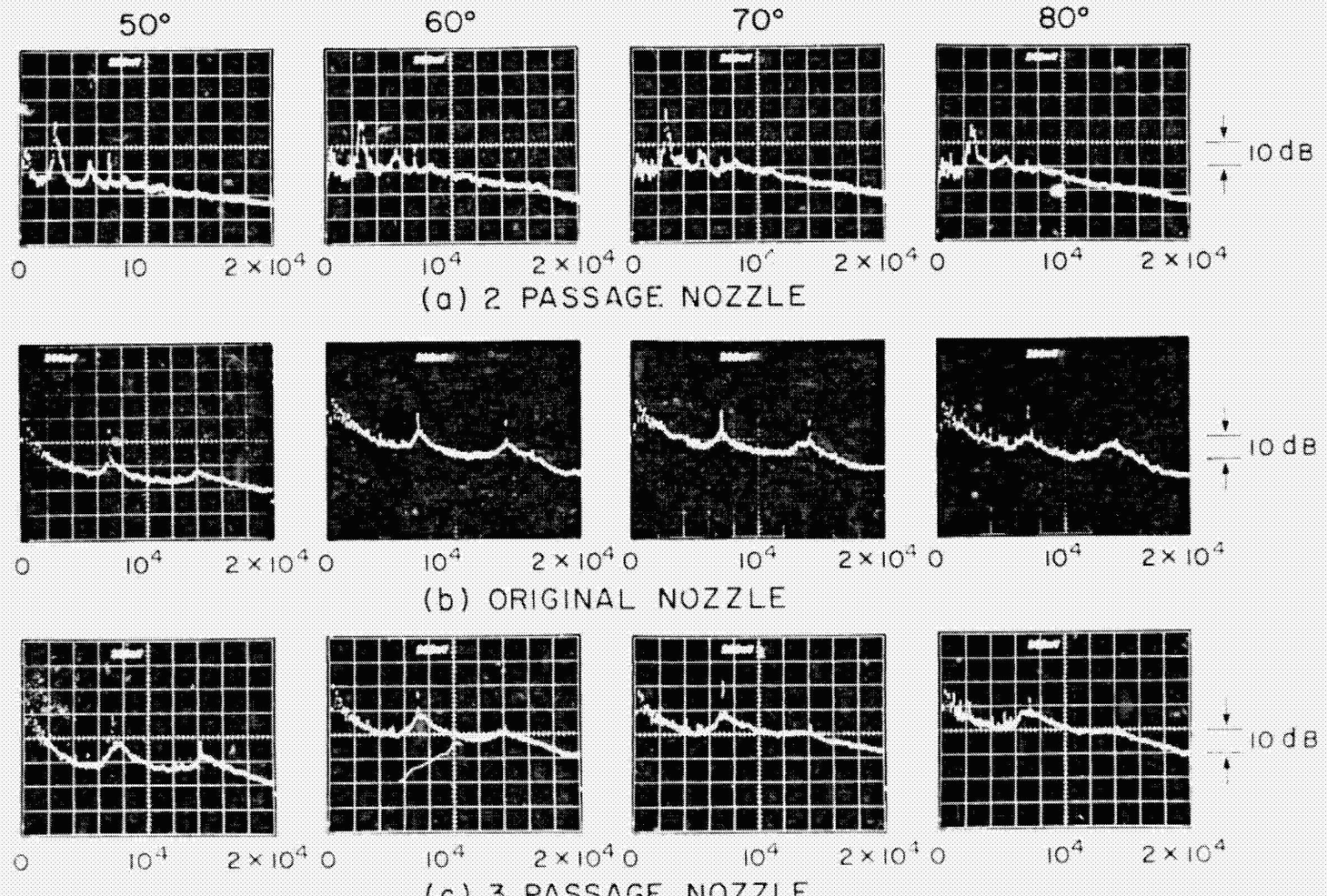
50°
60°
70°
80°
10 dB
0
10
2 × 10⁴
10⁴
(a) 2 PASSAGE NOZZLE
(b) ORIGINAL NOZZLE
(c) 3 PASSAGE NOZZLE

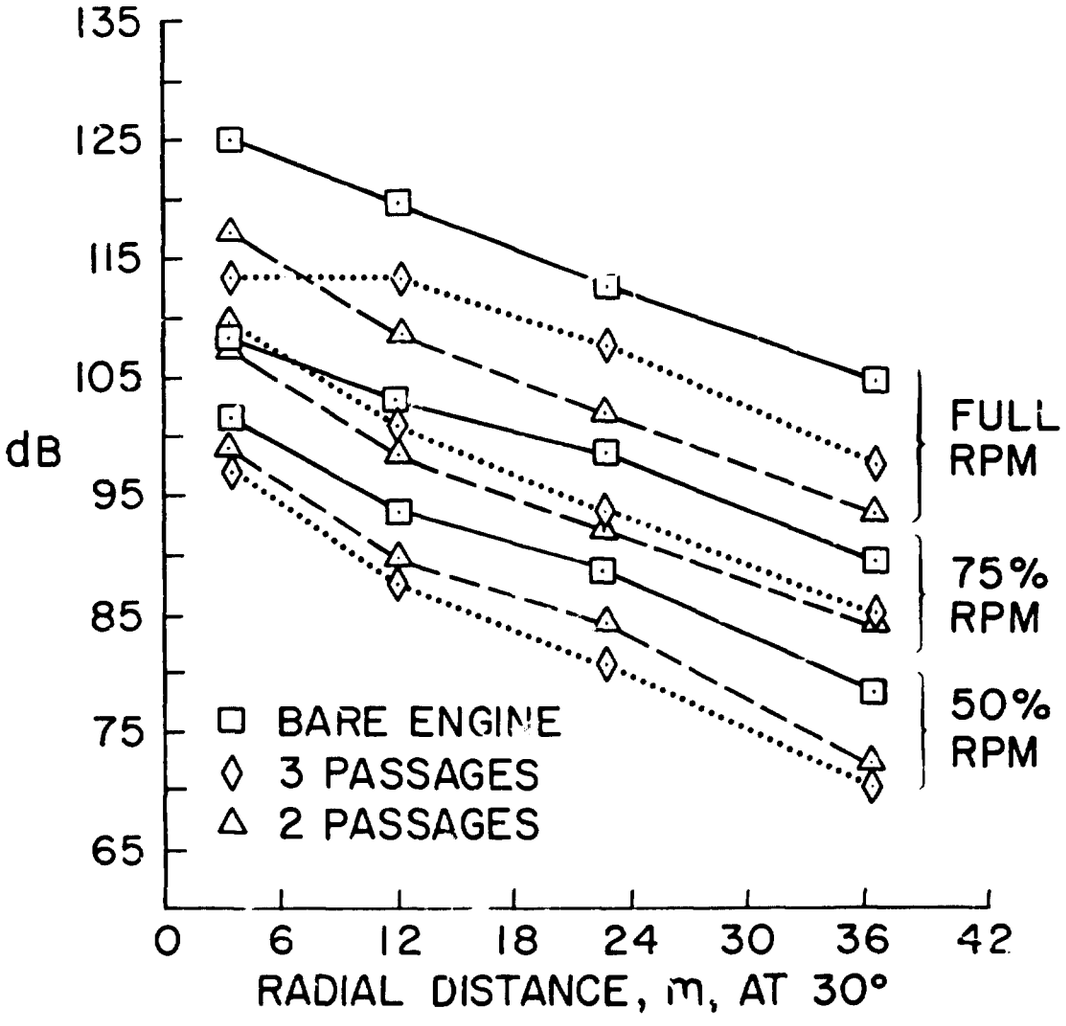
135
125
115
105
95
85
75
65
dB
FULL RPM
75% RPM
50% RPM
BARE ENGINE
3 PASSAGES
2 PASSAGES
0
6
12
18
24
30
36
42
RADIAL DISTANCE, m, AT 30°